Supplementary material

Logging Amazon forest increased the severity and spread of fires during the 2015-2016 El Niño

Paulo Eduardo Barni[a, *]
Anelícia Cleide Martins Rego[b]
Francisco das Chagas Ferreira Silva[b]
Richard Anderson Silva Lopes[c]
Haron Abrahim Magalhães Xaud[d]
Maristela Ramalho Xaud[d]
Reinaldo Imbrozio Barbosa[e]
Philip Martin Fearnside[f, g]

[a] Professor da Universidade Estadual de Roraima – UERR, *Campus* Rorainópolis
Av. Senador Helio Campos, s/nº, 69375-000, Rorainópolis, Roraima, Brazil.
pbarni@uerr.edu.br

[b] Graduados da Universidade Estadual de Roraima – UERR, *Campus* Rorainópolis
Av. Senador Helio Campos, s/nº, 69375-000, Rorainópolis, Roraima, Brazil.
{anelycia.com@gmail.com; chagasferreirasilva@gmail.com}

[c] Corpo de Bombeiros Militares de Roraima, Coordendoria Estadual de Proteção e Defesa Civil. Avenida Venezuela, 1271, 69309690 - Boa Vista, Roraima, Brazil. {raslopes@gmail.com}

[d] Empresa Brasileira de Pesquisa Agropecuária – Embrapa/RR. Rodovia BR 174, Km 8, Distrito Industrial. 69301-970, Boa Vista, Roraima, Brazil. {haronxaud@gmail.com; marisxaud@gmail.com}

[e] Instituto Nacional de Pesquisas da Amazônia (INPA), Rua Coronel Pinto, 315. CEP: 69301-150.   Boa Vista, Roraima, Brazil. reinaldo@inpa.gov.br

[f] Instituto Nacional de Pesquisas da Amazônia (INPA), Av. André Araújo, 2936. CEP: 69067-375, Manaus, Amazonas, Brazil. pmfearn@inpa.gov.br

[g] Brazilian Research Network on Global Climate Change – Rede Clima, Av. dos Astronautas, 1758 - Jardim da Granja, São José dos Campos – SP, 12227-010, Brazil

* Corresponding author

Supplementary material index:

1. Methodological procedures
1.1 Study area

Most of the study area (6402.6 km^2, or 96.2% of the study area) is in the municipality of Rorainópolis, followed by the municipality of São Luiz (164.2 km^2, or 2.4%) and the municipality of Caracaraí (90.5 km^2, or 1.4 %) (Table S1).

Table S1. Deforestation, forest fire, and logging in the portion of each municipality located in the study area.

Municipalities	Area (km^2)	% of the study area	Deforestation km^2	%	Forest fire (km^2)	% of the burned area	SL (km^2)	% of the logged area
Caracaraí	90.5	1.4	7.1	0.6	37.9	5.6	9.4	1.5
Rorainópolis	6,402.6	96.2	1,045.3	94.8	638.3	93.6	624.4	96.8
São Luiz	164.2	2.4	49.7	4.5	6.0	0.9	10.9	1.7
Total	**6,657.3**	**100.0**	**1,102.1**	**100.0**	**682.2**	**100.0**	**644.8**	**100.0**

1.2 Forest inventory locations

The locations and other information for plots sampled in the field are presented in Table S2. All plots measured 4 × 250 m (1000 m^2).

Table S2. Location (latitude and longitude), area (ha) and date of field data collection. SL=Selective Logging. Wo-SL = without selective logging. W-SL = with selective logging.

Plot name	SL	Latitude	Longitude	Area (ha)	*AGB_stock (Mg ha^{-1})	Fire	Census date (mm/dd/yyyy)
Plot 1	W-SL	0.930891	-60.451279	0.1	404.6	yes	03/11/2016
Plot 2	W-SL	0.932695	-60.447959	0.1	221.5	yes	03/11/2016
Plot 3	W-SL	0.929629	-60.442604	0.1	458.5	yes	03/16/2016
Plot 4	W-SL	0.927556	-60.441827	0.1	322.0	yes	03/16/2016
Plot 5	W-SL	0.934315	-60.449995	0.1	640.2	yes	03/16/2016
Plot 6	W-SL	0.934234	-60.452384	0.1	834.0	yes	03/16/2016
Plot 7	W-SL	0.909708	-60.452814	0.1	320.1	yes	03/23/2016
Plot 8	W-SL	0.906816	-60.453078	0.1	567.2	yes	03/23/2016
Plot 9	W-SL	0.912540	-60.452564	0.1	1095.4	yes	03/23/2016
Plot 10	W-SL	0.913743	-60.454606	0.1	427.1	yes	03/23/2016
Plot 11	W-SL	0.711231	-60.565005	0.1	863.9	yes	03/30/2016
Plot 12	Wo-SL	0.707785	-60.510418	0.1	289.6	yes	03/30/2016
Plot 13	Wo-SL	0.709255	-60.508096	0.1	504.0	yes	03/30/2016
Plot 14	W-SL	0.709511	-60.567284	0.1	1044.2	yes	03/30/2016
Plot 15	W-SL	0.712057	-60.587902	0.1	387.6	yes	03/30/2016
Plot 16	W-SL	0.712389	-60.591582	0.1	424.0	yes	03/30/2016
Plot 17	Wo-SL	0.989933	-60.425055	0.1	546.6	yes	04/06/2016
Mean	**-**	**-**	**-**	**-**	**550.0**	**-**	**-**

*Aboveground dry biomass stock based on Higuchi et al. (1998) with adjustment for 40% water content (Higuchi et al., 1998) and for biomass of palms (Saldarriaga et al., 1988).

1.3 Biomass calculation in inventory plots for deriving fractions of biomass killed

Unlike the biomass map for Roraima, which used the Barni et al. (2016) analysis with species specific data, only about half of the trees in the plots had known identities, and we therefore used the Higuchi et al. (1998) equation to calculate fresh biomass directly from DBH without using species-specific wood-density data. Because the plot data are only used for deriving the fractions of biomass killed by the fire in the different severity classes, not the forest

biomass to which these fractions will be applied, the use of different biomass estimation equations will not affect the results for the impact of fire in the study area, since the both the numerator and the dominator in the fractions of biomass killed have been calculated with the same method.

Fresh weight was converted to dry weight by multiplying by 0.60, which was the dry weight to fresh weight ratio derived by Higuchi et al. (1998: Table 3b). This rate was applied to the fresh-biomass value calculated by the Higuchi et al. (1998) equation for each tree in the database. This procedure was performed from the excel spreadsheet. Thus:

$$\text{Ln(Fresh weight)} = -1.497 + 2.548 \times \text{Ln(DBH)}$$
$$\text{Dry weight} = \text{EXP(Ln (Fresh weight))} \times 0.6$$

The total weight (kg^{-1}) of each plot (sum of the dry weight of all trees in the plot) was multiplied by 10 (to transform from kg^{-1} per plot to $kg\ ha^{-1}$) and, in sequence, the total weight in $kg\ ha^{-1}$ was divided by 1000 to transform into $Mg\ ha^{-1}$.

1.4 Area (ha) and volume (m^3) authorized in "alternative land-use" projects

The largest area authorized for deforestation (3300.7 ha, or 26.4% of the total area authorized) was in 2015 and the smallest (290.6 ha, or 2.3%) was in 2011. Only 26.2% (3114.1 ha) of these areas authorized for alternative land use were effectively deforested by 2019 (Table S3).

Table S3. Area and volume of wood authorized for harvest in alternative land-use projects in the study area.

Year	n	Authorized area (ha)	Authorized volume (m^3)	Average volume ($m^3\ ha^{-1}$)	*Deforestation (ha)	%	**YARSL (n)
2010	9	2,095.4	133,939.0	63.7	525.9	25.1	2.8
2011	2	290.6	13,027.8	49.5	102.4	35.2	4
2012	17	3,244.9	150,319.5	50.6	755.5	23.3	2
2013	4	873.2	46,156.7	53.3	195.0	22.3	1
2014	12	2,676.1	114,311.9	43.0	695.8	26.0	1
2015	14	3,300.7	153,920.6	48.4	839.7	25.4	4
Total	**58**	**12,480.9**	**611,675.5**	**51.4**	**3114.1**	**26.2**	**2.5**

* Deforestation by 2019.
** Years after the release to SL.

1.5 "Sustainable Forest Management" Plans

The areas released for selective logging in "sustainable forest management" plans in Rorainópolis totaled 11,958.8 ha from 2016 to 2020 with an average authorized harvest of 23.9 $m^3\ ha^{-1}$. In this area, a total volume of 281,091.3 m^3 of wood in logs was released (Table S4).

Table S4. Location (latitude and longitude), area (ha) and volume (m^3) authorized for logging in "sustainable forest management" plans in the municipality of Rorainópolis.

ID	Latitude	Longitude	Authorized area (ha)	Authorized volume (m^3)	Average volume (m^3 ha^{-1})	Year
1	0.4351889	-60.4069556	552.6	13,079.7	23.7	2019/20
2	0.3815278	-60.6354444	957.9	14,712.8	15.4	2017/18
3	0.5415483	-60.4245542	1,442.9	35,830.9	24.8	2019/20
4	0.7514861	-60.6653361	1,254.1	19,664.6	15.7	2018/19
5	0.5598333	-60.3416111	1,071.0	22,125.1	20.7	2018/19
6	0.7100000	-60.0663889	987.9	26,066.4	26.4	2016/17
7	0.5574109	-60.6592349	964.3	24,456.3	25.4	2020/21
8	0.2734927	-60.4002495	1,163.9	33,588.1	28.9	2020/21
9	0.5218820	-60.6587190	947.7	22,580.0	23.8	2020/21
10	0.9931272	-60.5705950	192.6	5.570.0	28.9	2020/21
11	0.2588300	-60.4437717	1,089.9	31,847.2	29.2	2020/21
12	0.4905078	-60.3520806	666.4	17,003.1	25.5	2020/21
13	0.4905078	-60.3520806	667.8	14,567.1	21.8	2020/21
	Total		**11,958.8**	**281,091.3**	**23.9**	

1.6 Fire severity estimation by NDVI and NBR

The results of the comparison between NDVI and NBR using fire-severity classes (light, moderate, strong and very strong) are presented in Table S5. Figure S1 shows the results of the comparative analysis between the NDVI and the NBR in the assessment of burned areas. Figure S2 shows a portion of the study area with fire-severity classifications by each index.

The larger area that the NBR index detected in the lowest severity class (light), as compared to NDVI, is an indication in favor of NDVI as a more accurate index for our purposes. The fires in the area occurred from 1 December 2015 to 23 March 2016, with most of the 216 "hot pixels" detected by the Aqua satellite being detected between 15 January and 5 February 2016. This means that the bulk of the burning was almost five months before the satellite pass on 9 June 2016, and, with the rainy season beginning at the end of March, there were over two months of rain before the satellite pass. Therefore there had been time for regeneration of green vegetation in the understory of the burned areas. The burn-severity classification by the sensors would be most likely to downgrade the assignment of values in lower severity classes, such as classifying a "moderate" burn as "light," because the more-severe burns would inhibit regeneration. The close agreement between the two indices (9,6% NDVI and 8.6% NBR) in their findings for the highest severity class (very strong) can be explained by the almost total inhibition of regeneration in these places when fire is very intense. In this case, the intensity of the fire may have partially or totally eliminated the seed bank from the soil, thereby making more time necessary for regeneration (Figure S2).

NDVI and NBR use different bands, which may have made the green regeneration lead NBR to downgrade the assigned severities more than did NDVI. NDVI uses Landsat 8 sensor bands 5 (near infrared [NIR] wavelength range: 0.851 - 0.879 micrometers) and 4 (red: 0.636 - 0.673 micrometers). NBR uses bands 7 (short-wave infrared 2 [SWIR2]: 2.107 – 2.294 micrometers) and 5 (NIR: 0.851 - 0.879 micrometers). In the case of NBR, there is an increase in the contrast between the values of photosynthetically active vegetation and photosynthetically inactive vegetation (dead biomass). Higher reflectance levels associated with photosynthetically active vegetation, and part of this increase in "greenness" detected by NBR, can be attributed to forest regeneration by sprouting, seedling emergence from the soil seed bank and appearance of herbaceous plants in abundance.

Both indices capture the "greenness" effect, but this reflection is not very evident in the case of NDVI because this composition uses band 4 (red). When using band 7 to compose the NBR there is a greater expansion of the values due to the greater contrast (greater difference) between the reflection values of bands 5 and 7 than between the reflection values of bands 5 and 4 used to compose the NDVI. For example, in our study the range of the NBR index values was 0.5010 (0.7205 minus 0.2104: Table S5) while the range of the NDVI was 0.3784 (0.6031 minus 0.2247: Table 1 in the main text). This difference meant a 32.4% increase in the amplitude of the NBR values in relation to the amplitude of the NDVI values.

This explanation is speculative due to the lack of information linking ground-level regeneration with the NBR index. Our empirical experience suggests rapid regeneration in lower-severity burns. This subject should be the object of future studies in the region due to the importance of improving forest degradation estimates.

Table S5. Comparison analysis between NDVI and NBR using fire-severity classes.

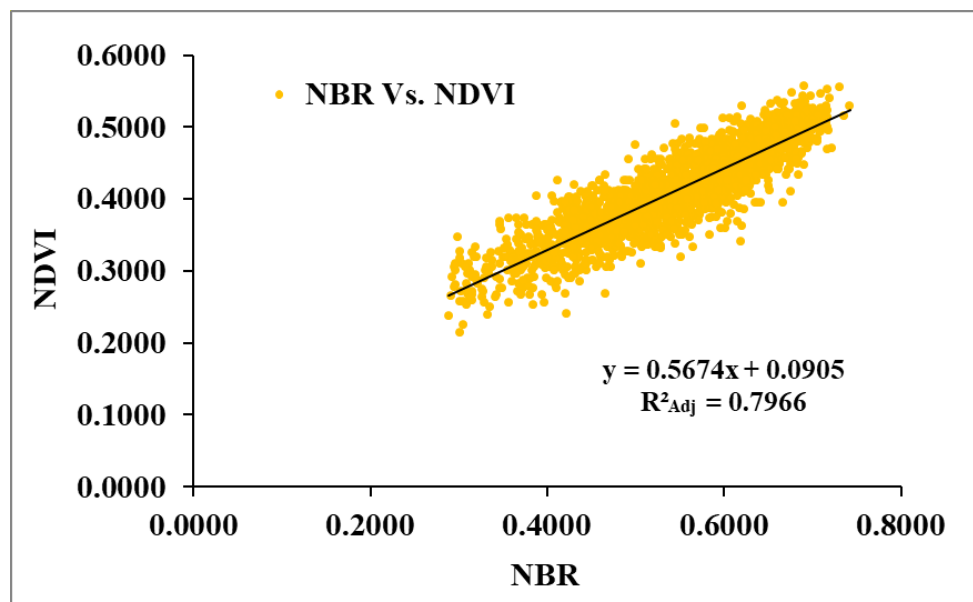| Class	NDVI Area (km^2)	%	NBR Area (km^2)	%	NDVI-NBR Area (km^2)	%	NBR values Dimensionless (- 1 to +1)
Light	246.5	36.2	283.6	41.6	-37.1	-15.1	0.5764 to 0.7205
Moderate	229.0	33.5	208.4	30.6	20.6	9.1	0.4904 to 0.5764
Strong	140.7	20.7	130.7	19.2	10.0	7.1	0.3944 to 0.4904
Very strong	64.9	9.6	58.4	8.6	6.5	10.0	0.2104 to 0.3944
Total	**681.1**	**100.0**	**681.1**	**100.0**	**0.0**	**-**	**-**

Figure S1. Comparison between sample values (n = 2502) for NBR and NDVI in burned areas in the study area.
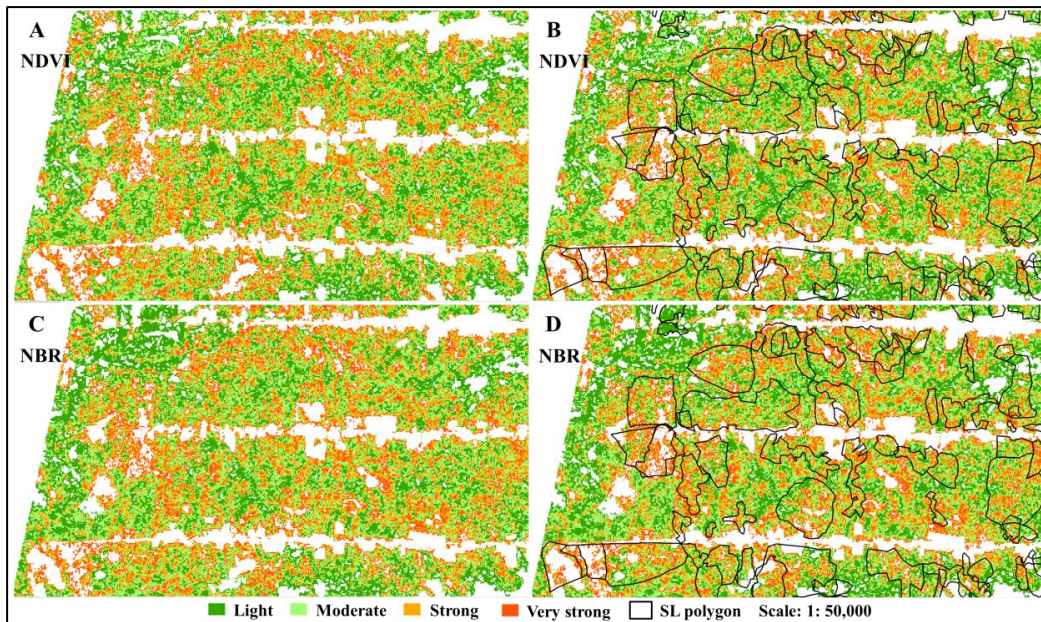
Figure S2. Fire severity classification using NDVI (A and B) and NBR (C and D) in a portion of the study area.

1.7 Wood density

The values calculated for the basic density of wood (g cm^{-3}) harvested in the SL areas are shown in Table S6. The table also provides the sources of the information.

Table S6. Calculation of weighted mean wood density.

Species	Local name	Wood volume (1)		Basic density	Note	Weighted	Density
		m³	%	(g cm^{-3})			Source
Manilkara huberi	Maçaranduba	9,806	29.2	0.878	(2)	0.257	Silveira et al., 2013
Dinizia excelsa	Angelim-ferro	9,235	27.5	0.86		0.237	Fearnside, 1997
Hymenolobium excelsum	Angelim-pedra	4,440	13.2	0.64		0.085	Fearnside, 1997
Goupia glabra	Cupiúba	3,880	11.6	0.712	(2,3)	0.082	Nogueira et al., 2005
Erisma fuscum	Caferana	2,170	6.5	0.49	(4)	0.032	Fearnside, 1997
Qualea paraensis	Rabo-de-arraia	1,350	4.0	0.67		0.027	Fearnside, 1997
Protium sp.	Casca-grossa	1,000	3.0	0.589	(2,3,5)	0.018	Nogueira et al., 2005
Clarisia racemosa	Guaruba	1,000	3.0	0.665	(2)	0.020	Silveira et al., 2013
Couratari stellata	Tauari	320	1.0	0.63		0.006	Fearnside, 1997
Bagassa guianensis	Tatajuba	280	0.8	0.69		0.006	Fearnside, 1997
Handroanthus sp.	Ipê	77	0.2	0.91		0.002	Fearnside, 1997

(1) Wood volumes are from a 2013 survey of 9 sawmills in Rorainópolis by Crivelli et al., 2017).
(2) Includes variation along the trunk.
(3) Includes radial variation (density of cross-sectional discs, including bark)
(4) Density of a congeneric.
(5) Mean of 14 trees from 7 species.

1.8 Estimation of harvesting intensity and loss of live biomass from cumulative selective logging by 2015

Only an approximate value can be estimated for the loss of live biomass to selective logging at the time of the 2015-2016 fires. Official data on log volumes processed in sawmills and

authorized for sale have wide discrepancies, and data are only available for certain years for different measures (Table S7). The data for log volume processed in sawmills, which information is available for the most years (2007-2019) is particularly unreliable. From 2007 to 2014 the volume officially reported (Brazil, IBGE, 2021) averaged 34,525 m^3 year^{-1}, jumping by 5.3 fold in 2015 to a new level, presumably due to an improvement in the veracity of reporting beginning in 2015. The new level presumed to originate in the municipality of Rorainópolis (90%, see text) is close (4.5% below) to the amount authorized for sale from clearcutting projects in 2015, the only year with data on the clearcutting projects after this shift (data on clearcutting projects are available for 2010-2015). The volume data for clearcutting authorizations therefore appears to be a good representation of the portion (estimated at 90%) of volume processed by sawmills in Rorainópolis that originates within the municipality and therefore in the 520.5-km^2 area where we mapped selective logging. During the 6 years with data for authorizations of clearcutting projects (2010-2015) the mean amount authorized was 101,945.8 m^3 year^{-1}. From this 1.2% must be deducted for the logs that were sold from the areas that were authorized for clearcutting that were, in fact, actually clearcut (see text), meaning that the volume harvested through selective logging was 100.742.5 m^3 year^{-1}. If one considers that this annual harvest also applies to the preceding 4 years (2006-2009), when substantial logging activity is known to have taken place, then the harvest intensity considering the 10-year 2006-2015 period was 19.4 m^3 ha^{-1}. Considering the mean basic density the wood of 0.770 (See text Section 2.3.2), this removal in logs represents 14.9 Mg ha^{-1}. To obtain the reduction in live biomass from the selective logging we must also include the stumps and crowns of the harvested trees, as well as the biomass of unharvested trees killed from damage in the logging operations. Nogueira et al. (2008) found that stumps represented 1% of the biomass of the commercial boles in 264 harvested trees in Brazil's "arc of deforestation" in the southern part of Brazilian Amazonia. Applying this percentage, the stumps represent 0.15 Mg ha^{-1}, and the trunk from the ground to the first significant branch for the harvested trees represents 15.05 Mg ha^{-1}. Crowns were found to represent an average of 30.8% of the aboveground biomass in 121 trees in dense forest near Manaus (da Silva, 2007, p. 57). The crowns of the harvested trees therefore represent 6.7 Mg ha^{-1}, and the total (commercial log + stump + crown) represents 21.75 Mg ha^{-1}. Since this illegal selective logging does not employ reduced-impact techniques, damage equal to 64% of the harvested biomass is considered, based on studies reviewed in Fearnside (1995, p. 321). This increases the aboveground biomass loss to 35.67 Mg ha^{-1}.

Table S7. Comparison of official data sources on log volumes in Rorainópolis

Year	Volume processed in sawmills (m³) (a)	Processed log volume assumed to come from Rorainópolis (m³) (b)	Volume authorized in deforestation projects (m³) (c)	Volume authorized in forest-management projects (m³) (d)	Discrepancy between processed volume assumed to come from Rorainópolis and volume authorized in deforestation projects (m³)	(%)
2007	40,000	36,000				
2008	32,700	29,430				
2009	32,500	29,250				
2010	33,000	29,700	133,939.0		104,239.0	351.0
2011	32,600	29,340	13,027.8		-16,312.2	-55.6
2012	35,000	31,500	150,319.5		118,819.5	377.2
2013	36,400	32,760	46,156.7		13,396.7	40.9
2014	34,000	30,600	114,311.3		83,711.3	273.6
2015	179,147	161,232	153,920.6		-7,311.7	-4.5
2016	193,210	173,889		20,066.4		
2017	424,601	382,141		14,712.8		
2018	155,942	140,348		41,789.7		
2019	170,000	153,000		13,079.7		
2020				149,611.8		
2010-2015		315,132.3	611,674.9		296,542.6	94.1
2010-2014		153,900	457,754.0		303,854.3	197.4

(a) Brazil, IBGE (2021).
(b) Assumed 90% originates from the municipality of Rorainópolis and 10% from the neighboring municipality of Caracaraí and São Luiz. Volume from indigenous areas is assumed not to be reported.
(c) Table S3.
(d) Table S4.

1.9 Selective logging
1.9.1 Mapping of the selective logging

For mapping selective logging, 16 images were used: 10 images from Landsat 5 TM and six from Landsat 8 OLI / TIRS (Table S8). The classification was checked by field observations in burned and unburned areas in 21 inventoried plots after the fires occurred (Barni et al., 2017), of which 17 were used in the present study. We also used a vector file (shapefile) provided by FEMARH for areas licensed for deforestation (128.3 km^2) in our study area during the same period of analysis (2007 to 2015) as a way to resolve doubts about spectral patterns in the images caused by SL. After mapping SL for this interval, the vector files were gathered in a single vector layer, converting this to an SL map (Figure S3).

Table S8. Mapping of selective logging (SL) from 2007 to 2015 in the study area.

*Year	Image date	**Satellite data	SL (km²)	%	***Deforestation (km²)	%
2007	21 Sept.	Landsat 5	39.7	6.2	19.4	11.3
2008	10 Nov.	Landsat 5	37.6	5.8	26.3	15.3
2009	29 Nov.	Landsat 5	46.9	7.3	18.2	10.6
2010	15 Oct.	Landsat 5	75.9	11.8	16.1	9.3
2011	31 Aug.	Landsat 5	80.4	12.5	11.2	6.5
2012	–	–	–	–	15.5	9.0
2013	23 Oct.	Landsat 8	72.4	11.2	22.8	13.2
2014	29 Dec.	Landsat 8	93.1	14.4	19.5	11.3
2015	30 Nov.	Landsat 8	198.7	30.8	23.3	13.5
TOTAL	16	–	644.8	100.0	172.3	100.0

* No images were observed for the year 2012 in our study area.
** RGB and NDVI images.
*** Deforestation in the municipality of Rorainópolis (Brazil, INPE, 2020).
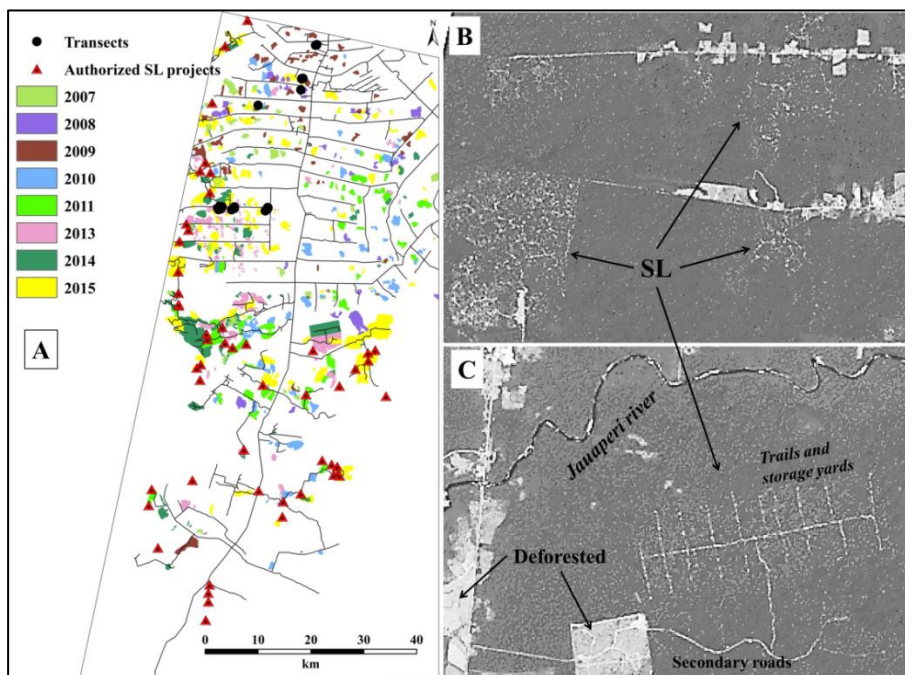

Figure S3. (A) Selective-logging map from 2007 to 2015 with the location of the 17 transects from the forest inventory and SL projects authorized by FEMARH in the study area, and in (B) and (C) detection of the SL areas in the RGB and NDVI images (Scale: 1: 50,000).

1.9.2 Severity of fire according to the year of selective logging

Analysis of the fire severity classes in areas impacted by SL showed that the class with the greatest severity ("very strong") increased with decreasing time elapsed between the harvesting of wood and the occurrence of the fire. For example, for areas logged in 2007 the difference between the "light" and "very strong" classes was 7.4%, while for areas logged in 2015 (the year the fire started in the region) this difference was ~ 3 times greater (21.9%) (Table S9).

Table S9. Severity of fire according to the year of selective logging

Year	Light Area (km²)	%	Moderate Area (km²)	%	Strong Area (km²)	%	Very strong Area (km²)	%	Total
2007	5.5	10.8	6.1	10.4	4.5	10.0	3.0	11.6	**19.1**
2008	3.3	6.4	3.0	5.2	1.9	4.2	0.8	2.9	**8.9**
2009	7.1	13.9	7.6	13.0	4.8	10.5	2.1	8.1	**21.5**
2010	6.0	11.8	5.0	8.7	2.7	6.0	0.9	3.6	**14.7**
2011	3.7	7.2	4.0	6.9	2.9	6.4	1.4	5.3	**11.9**
2013	4.7	9.3	7.4	12.7	6.8	15.1	3.9	14.8	**22.8**
2014	4.6	9.1	6.8	11.7	6.5	14.4	3.9	15.1	**21.9**
2015	16.0	31.5	18.3	31.4	15.1	33.5	10.0	38.4	**59.5**
Total	**51.0**	**100.0**	**58.2**	**100.0**	**45.2**	**100.0**	**26.1**	**100.0**	**180.5**

1.10 Calculation of weights-of-evidence
1.10.1 *A priori* probabilities of fire events

The weights-of-evidence originated from the Bayesian method of calculating conditional probabilities. Its application in modeling the dynamics of land-use and land-cover change assumes that it is possible to calculate the probability *a posteriori* of an event happening based on information obtained *a priori* from a set of conditions (evidence) that favored or determined the event in question. In our study, a set of conditions or "evidences" was transformed into maps of distance variables (maps of continuous variables) and maps of categorical variables (maps of classes) to represent influences on the occurrence of forest fires in the study area in 2015/2016 (Figure S4). The calculations of the weights-of-evidence and of the probability map were carried out in a sub-model in the Dinamica-EGO software with a stacking of the maps (Soares-Filho et al., 2014) (Figures S5 and S6).
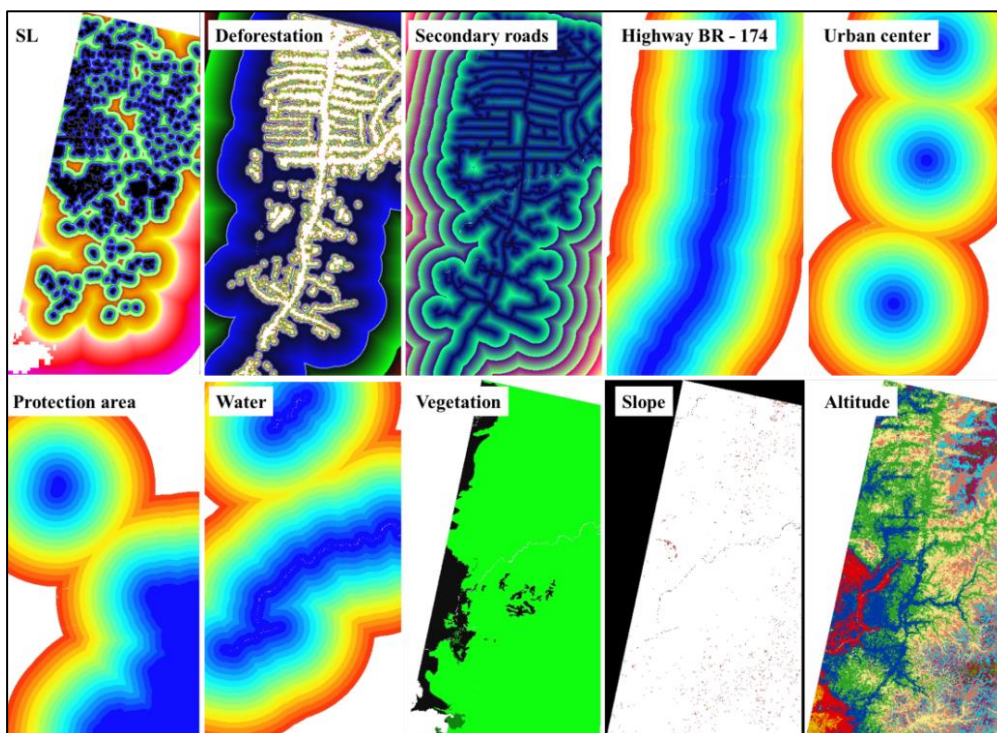

Figure S4. Set of continuous variables (with distance ranges) and categorical variables (vegetation, slope and altitude). SL = selective logging.
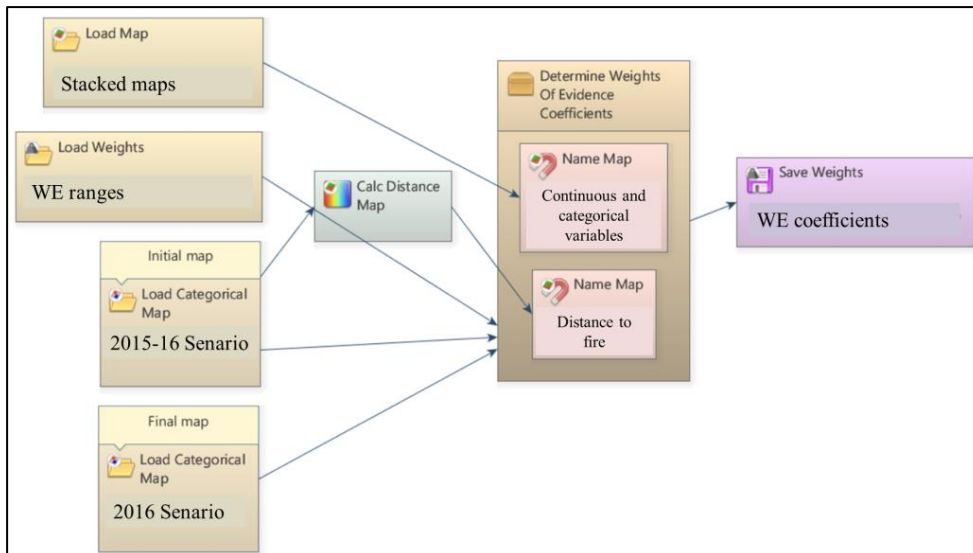
Figure S5. Submodel of the Dinamica-EGO software for calculating the weights-of-evidence coefficients. **Source**: adapted of the Dinamica-EGO guidebook (https://csr.ufmg.br/dinamica/).
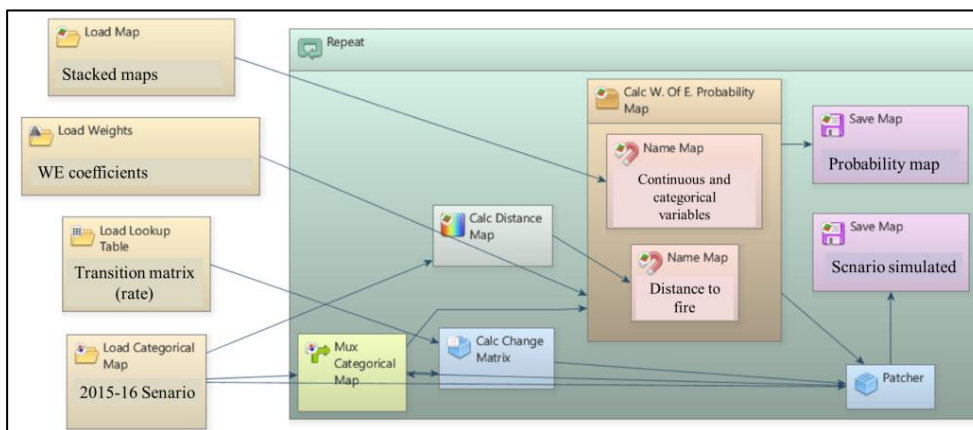

Figure S6. Submodel of the Dinamica-EGO software for calculating the map of transition probabilities and the simulated fire map. **Source**: adapted of the Dinamica-EGO guidebook (https://csr.ufmg.br/dinamica/).

The influence of the weights-of-evidence can be positive or negative. The coefficients of the weights-of-evidence are positive when they favor or promote an increase in the probability of a class transition, and they are negative when they inhibit the class transition, decreasing its probability of occurrence. For example, the spatial probability map (derived from weights-of-evidence) will indicate to the software which sets of pixels representing forest on a land-use map at time t_1 have a greater chance or probability of changing to a burnt area at time t_2. The variable "distance to secondary roads," for example, will have its maximum positive (+) weight-of-evidence in the first meters away from the fire, and at progressively greater distances this influence will decrease until it becomes negative (-), reaching its negative maximum at the most distant point.

In the modeling the weights-of-evidence represent the amount of influence of each variable on the probability of transition of a cell representing a particular state (i: forest) to change to another state (j: fire (F)), depending, for example, on its location within a distance range. In this way, the cell that is located closest to where the phenomenon occurred has a higher chance or greater probability. This relationship can be represented by equations (1) to (9) below, derived from the Bayesian inference method:

$$P(F/A) = \frac{P(F \cap A)}{P(A)} \qquad (1)$$

$$P(A/F) = \frac{P(A \cap F)}{P(F)} \qquad (2)$$

$$P(A \cap F) = P(A/F) * P(F) \qquad (3)$$

Likewise, considering non-event F, as not F ($\hat{F}$), we obtain (4):

$$P(\hat{F}/A) = P(\hat{F}) * \frac{P(A/\hat{F})}{P(A)} \qquad (4)$$

Now replacing (4) in (1), we have (5):

$$P(F/A) = P(F) * \frac{P(A/F)}{P(A)} \qquad (5)$$

Applying the ratio between Equations (6) and (7), we obtain (8): (6)

$$O(F/A) = O(F) * \frac{P(A/F)}{P(A/\hat{F})} \qquad (6)$$

$$\log O(F/A) = \log O(F) + \log \frac{P(A/F)}{P(A/\hat{F})} \qquad (7)$$

$$\log O(F/A) = \log O(F) + W^+ \qquad (8)$$

Thus:

$$\log O(F/A) = \log O(F) + \sum_{i=1}^{n} W_i^+ \qquad (9)$$

Where "{F}" and "O {F / A}" are proportions of *a priori* probability that the "F" (fire) event occurs, and the fire event occurs given a spatial pattern "A", respectively. "W +" is, therefore, the weight-of-evidence of event F occurring given the spatial pattern "A". Thus, the calculation of the *a posteriori* spatial transition probability "i → j" for a spatial data set "(B, C, D, ... N)" can be represented by (10):

$$P(i \to j/B \cap C \cap D ... \cap N) = \frac{e^{\sum W_i^+}}{1 + e^{\sum W_i^+}} \qquad (10)$$

Where, "B, C, D, ..., N" are values of the k spatial variables estimated at positions "x, y", being represented by their respective weights-of-evidence "W + N". For more details on the weights-evidence method, see Barni et al. (2015).

1.10.2 Correlation between spatial variables in the calculation of weights-of-evidence

Application of the weights-of-evidence method presupposes spatial independence between variables. In the case of pairs of variables with a correlation above 0.5, one of them must be removed from the set of maps that will be used in the modeling in order to guarantee compliance with the model's assumption of independence (Bonham-Carter, 1994). This independence is

measured or estimated by observing some parameters, mainly that of contingency, which, like Pearson's correlation analysis (Figueiredo-Filho and Silva Junior, 2009), indicates the amount of correlation that exists between two spatial variables (Table S10).

Table S10. Correlated variables in the calculation of the weights of evidence.

Variable 1	Variable 2	CHI Sq.	CRAMMER	CONTING	ENTROPY	INF_C*INCERT
Deforestation	Secondary roads	26324385.8	0.38	0.86	4.36	0.35
Fire	Deforestation	13591362.2	0.31	0.81	4.97	0.20
SL	Secondary roads	11137374.0	0.30	0.78	4.75	0.21
BR-174	Village	12300562.7	0.29	0.78	4.74	0.24
Fire	SL	10654858.5	0.26	0.77	5.07	0.18
Fire	Secondary roads	10387346.3	0.29	0.77	5.04	0.18
Deforestation	SL	9312302.5	0.26	0.75	4.87	0.17
BR-174	Secondary roads	7309303.3	0.22	0.68	4.88	0.14
BR-174	Deforestation	7117818.5	0.21	0.67	4.88	0.14
Fire	Protected area	4585235.4	0.20	0.65	5.02	0.13
Fire	BR-174	5084155.0	0.20	0.65	5.22	0.09
Protected area	SL	4263722.4	0.19	0.64	4.83	0.13
Protected area	BR-174	4550167.7	0.19	0.63	4.80	0.13
Secondary roads	Village	4673617.7	0.19	0.61	5.07	0.11
Deforestation	Village	4629794.4	0.18	0.61	5.09	0.10
BR-174	SL	3819157.9	0.17	0.59	5.06	0.07
Protected area	Altitude	3321756.0	0.23	0.59	4.28	0.12
Fire	Village	3152213.0	0.14	0.57	5.35	0.07
SL	Water	2948194.9	0.15	0.56	5.14	0.06
Protected area	Secondary roads	3536961.0	0.16	0.56	4.90	0.09
Protected area	Deforestation	3378198.9	0.15	0.55	4.93	0.09
Protected area	Village	2480305.7	0.14	0.53	5.06	0.07
Protected area	Water	2553570.6	0.14	0.52	4.96	0.08
Water	Altitude	2382190.2	0.19	0.52	4.64	0.07
Altitude	Vegetation	2335823.6	0.40	0.49	2.34	0.10
Secondary roads	Altitude	2291973.7	0.18	0.49	4.60	0.06
SL	Village	2019896.1	0.12	0.48	5.23	0.06
Water	SL year class	214633.3	0.21	0.48	4.20	0.06
Village	SL year class	211868.6	0.21	0.48	4.30	0.06
Protected area	SL year class	181646.8	0.20	0.47	4.06	0.08
BR-174	Altitude	1947197.2	0.17	0.46	4.58	0.06
Fire	Water	1609818.9	0.10	0.45	5.42	0.04
Deforestation	Water	2167922.4	0.11	0.45	5.25	0.05
Deforestation	Altitude	1804270.1	0.16	0.44	4.61	0.05
BR-174	SL year class	168417.7	0.18	0.44	4.18	0.05
Fire	Altitude	1596435.5	0.15	0.43	4.85	0.04
SL	Altitude	1589559.1	0.15	0.42	4.64	0.04
BR-174	Water	1463864.6	0.10	0.40	5.25	0.03
Fire	SL year class	133323.5	0.16	0.40	4.38	0.05
Village	Altitude	1239948.2	0.13	0.39	4.74	0.04
Water	Secondary roads	1464261.7	0.10	0.38	5.29	0.04
Deforestation	SL year class	111350.3	0.15	0.37	4.21	0.04
Water	Village	1102794.6	0.07	0.36	5.38	0.03
Water	Vegetation	771589.5	0.25	0.33	3.11	0.04

BR-174	Vegetation	798968.3	0.24	0.32	2.98	0.04
Slope	Altitude	838470.5	0.11	0.32	4.11	0.03
Protected area	Vegetation	654567.6	0.23	0.31	2.79	0.03
Secondary roads	SL year class	68851.5	0.12	0.30	3.87	0.02
SL year class	Altitude	68036.6	0.12	0.29	3.69	0.03
Secondary roads	Vegetation	475077.7	0.18	0.25	3.01	0.02
Village	Vegetation	440054.3	0.18	0.25	3.13	0.02
SL	Vegetation	444832.3	0.18	0.24	3.05	0.02
Deforestation	Vegetation	327915.6	0.15	0.21	3.00	0.02
Fire	Vegetation	323501.9	0.15	0.21	3.26	0.01
SL year class	Vegetation	26428.0	0.14	0.19	2.18	0.02
Protected area	Slope	221586.4	0.06	0.18	4.52	0.01
Water	Slope	203287.6	0.06	0.17	4.76	0.01
SL	Slope	154153.7	0.05	0.14	4.74	0.00
Secondary roads	Slope	145011.5	0.05	0.14	4.69	0.00
Deforestation	Slope	128456.0	0.04	0.13	4.68	0.00
BR-174	Slope	123456.6	0.04	0.13	4.66	0.00
Fire	Slope	91464.5	0.04	0.11	4.94	0.00
Slope	Vegetation	54819.5	0.06	0.09	2.46	0.00
Village	Slope	29033.2	0.02	0.06	4.80	0.00
SL year class	Slope	2855.3	0.02	0.06	3.98	0.00
SL	SL year class	0.0	0.00	0.00	1.93	0.00

SL = Selective logging

1.11 Model validation using an exponential decay function and fuzzy similarity

The "Calc reciprocal similarity map" function in Dinamica-EGO calculates a two-way similarity from the first map (simulated scenario) to the second (initial scenario) and from the second to the third (final scenario) (Figure S7). It is advisable to always chose the smaller similarity value since random maps tend to produce artificially high fits when compared univocally, because they spread the changes over the entire map. This test employs an exponential decay function truncated outside of a window size of 11×11 cells. The test result is returned in a .csv table file (Figure S8).
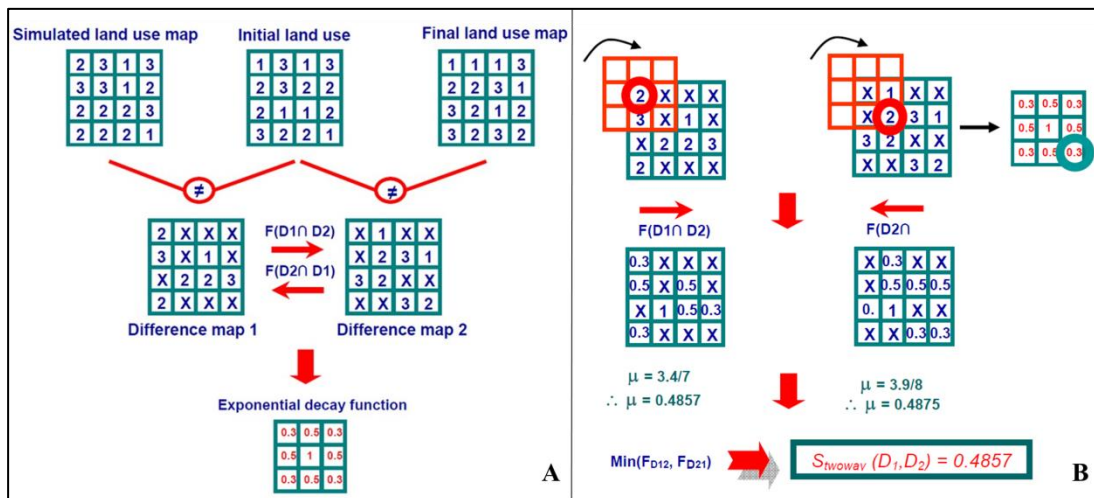

Figure S7. Fuzzy comparison method using a map of differences and an exponential decay function. The process applies a constant decay function in which all window weights are set to 1 (**A**). The window convolutes over the map, obtaining a fuzzy value for the central cell (**B**). X = null values in the map. **Source**: adapted from the Dinamica-EGO guidebook (https://csr.ufmg.br/dinamica/).
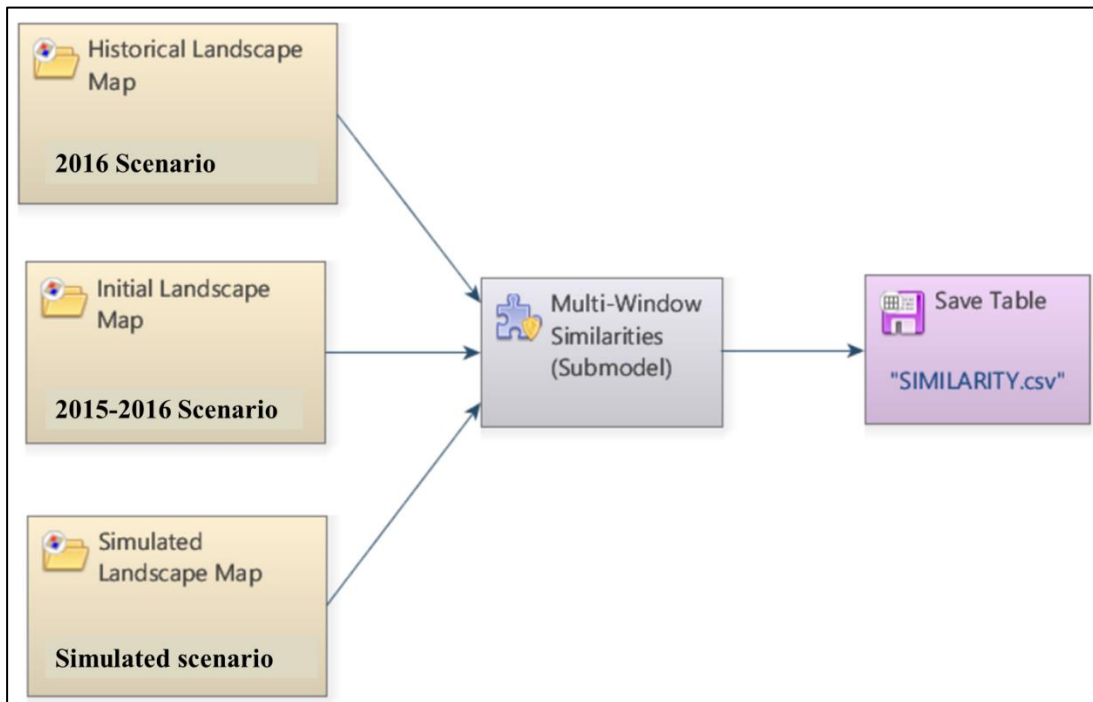
Figure S8. Submodel for similarity calculation in Dinamica-EGO software. **Source**: adapted from the Dinamica-EGO guidebook (https://csr.ufmg.br/dinamica/).

2. Results
2.1 Areas of occurrence

The areas of occurrence of the main variables distributed in the study area are presented in Table S11. The original forest area was estimated at 6512.4 km^2, representing 97.8% of the study area.

Table S11. Original forest area (km^2), protected areas, non-forest and deforestation occurring in the study area.

	Class	Area (km^2)	%	Forest fire (km^2)	Forest fire % of forest area	SL-fire (km^2)	SL-fire % of forest fire area	SL (km^2)	SL-fire (%) of SL area
Original vegetation	**Forest**	6,512.4	97.8						
	Non-forest	144.9	2.2						
	Total	**6,657.3**	**100.0**						
2016 vegetation	**Forest**	5,410.3	81.3	682.2	12.6	180.7	26.5	644.8	28.0
	Deforestation	1,102.1	16.6	–	–	–	–	–	–
	Non-forest	144.9	2.2	–	–	–	–	–	–
	Total	**6,657.3**	**100.0**						
Protected areas	**Indigenous land**	875.6	13.2	0.0	0.0	–	–	–	–
	Anauá National Forest	2.6	0.04	2.0	76.9	–	–	–	–

2.2 Estimates of biomass by forest type

Dense ombrophilous forest was the most affected by understory fires, totaling 532.7 km^2 and the estimated affected dry biomass at the time of the fire totaling 26.2×10^6 Mg. Ecotone forest had the smallest area (9.3 km^2) and the smallest amount (0.3×10^6 Mg) of affected biomass (Table S12).

Table S12. Estimated biomass before and after logging in the area affected by fire separated by forest type and by selective-logging status.

Forest	Original biomass (prior to logging)				Affected biomass (biomass at time of fire)					
	Total area affected by fire (km^2)	Total biomass in area affected by fire (10^6 Mg)	% of total biomass in area affected by fire	Mean original biomass (Mg ha^{-1})	Area W/SL (km^2)	Biomass after logging (10^6 Mg)	Biomass removed or killed by SL (10^6 Mg)	Affected biomass in area with SL (10^6 Mg)	Area Wo/SL (km^2)	Affected biomass in area Wo/SL (10^6 Mg)
Campinarana	140.0	3.6	13.2	255.6	28.3	0.71	0.1	0.7	111.7	2.9
Ecotone	9.3	0.33	1.2	360.3	0.0	0.0	0.0	0.0	9.3	0.3
Ombrophilous	532.7	23.2	85.6	435.3	152.3	6.63	0.5	6.1	380.3	16.6
Total	**681.9**	**27.1**	**100**	**397.4**	**180.6**	**7.3**	**0.6**	**6.7**	**501.3**	**19.8**

The estimation of forest biomass was performed for each forest type separately for areas with and without selective logging (SL). The dense ombrophilous forest (Ds) had the largest extension in terms of occupied area (87.8%) and in terms of biomass (92.5%) in relation to the total biomass (277.37×10^6 Mg) estimated for the original forest areas. The biomass of the areas under SL (27.6×10^6 Mg) represented 9.9% of the total biomass found in the study area, and 95.3% of that biomass was under dense ombrophilous forest (Table S13).

Table S13. Estimated biomass (Mg) in the study area separated by areas affected by selective logging (SL) (W-SL) and areas not affected by SL (Wo-SL).

Type	Area (km^2)	%	Biomass (10^6 Mg)	Mean (Mg ha^{-1})	Wo/SL 10^6 Mg	%	W/SL (10^6 Mg)	%
Campinarana	727.9	11.2	18.7	256.3	17.4	93.0	1.30	7.0
Ecotone	63.7	1.0	2.1	335.5	2.1	99.1	0.02	0.9
Ombrophilous	5,720.8	87.8	256.7	448.5	230.3	89.7	26.3	10.3
Total	**6,512.4**	**100.0**	**277.4**	**425.9**	**249.8**	**90.0**	**27.6**	**9.9**

Wo/SL = without selective logging. W-SL = with selective logging.

The cumulative loss of original biomass by deforestation up to 2016 was estimated at 48.04 $\times 10^6$ Mg, representing more than twice (2.1 times) the biomass affected by SL in our study area. The area deforested in dense ombrophilous forest (1059.3 km^2) represented 96.1% of the total area deforested by 2016 and 97.5% of the total biomass lost (Table S14).

Table S14. Biomass lost due to cumulative deforestation up to 2016.

Deforestation	Area (km^2)	%	Biomass (10^6 Mg)	%	Mean (Mg ha^{-1})
Campinarana	33.8	3.1	0.9	1.8	255.6
Ecotone	8.8	0.8	0.3	0.7	367.4
Ombrophilous	1,059.3	96.1	46.9	97.5	442.3
Total	**1,101.9**	**100.0**	**48.0**	**100.0**	**436.0**

2.3 Vulnerability of the forest to understory fires in SL areas

SL influenced the spread of fire in the study area during the 2015/2016 El Niño event within the fire-severity classes. Based on NDVI image analyses, the graphs in Figure S9 show positive correlations between fires and the logging practiced in years immediately prior to the fires.
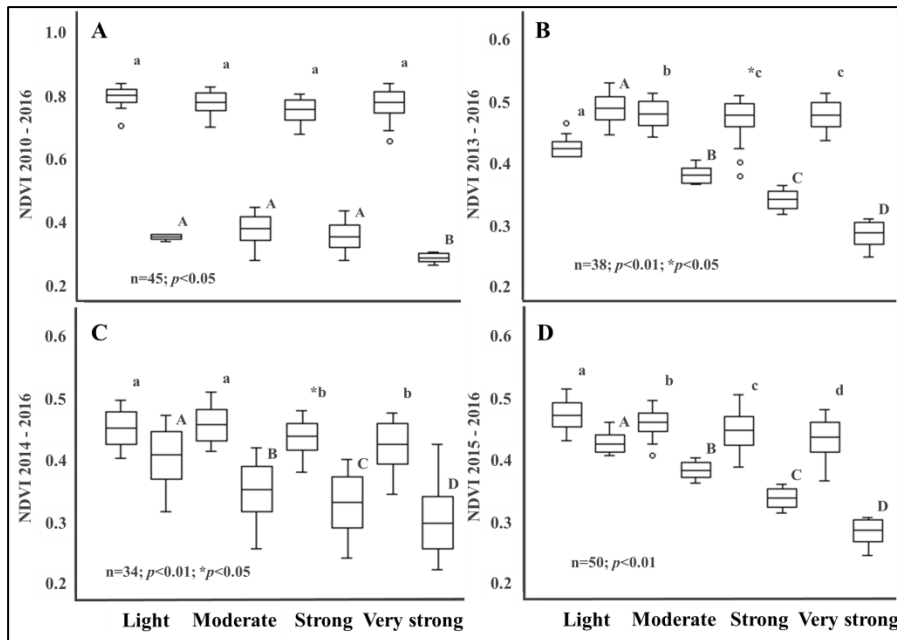
Figure S9. Comparison between NDVI values in SL areas in years prior to the fires with the NDVI values in the fire image for 2016. (A) Comparison of NDVI values between the years 2010 and 2016. (B) Comparison of NDVI values between the years 2013 and 2016. (C) Comparison of NDVI values between the years 2014 and 2016 and (D) comparison of NDVI values between the years 2015 and 2016. The lower-case letters above the boxes indicate statistical results between the NDVI values in years prior to the fires considering the fire-severity classes of the fires, while upper-case letters indicate the statistical results for the NDVI values in the 2016 image at the fire-event locations, also considering the severity classes.

2.4 Fire and SL behavior as a function of forest-edge distance

The highest occurrence of forest fires (114.9 km^2: 20.1%) in the study area was found in the range between 0 to 120 m from the forest edge. The SL presented a similar result reaching 113.9 km^2 (24.3%) in the first interval. The burned areas affected by SL were calculated at 161.2 km^2 in the range between 0 and 1200 m, representing 89.4% of the total reached in the study area (Table S15).

Table S15. Fire and SL occurrence depending on the distance from the forest edge.

Range (m)	Fire (km^2)	%	SL (km^2)	%	SL x Fire (km^2)	%	SL / Fire (%)	SL x Fire / Fire (%)	SL x Fire / SL (%)
0 -- 120	114.9	20.1	113.9	24.3	23.7	14.7	99.1	20.6	20.8
120 -- 240	95.3	16.7	58.2	12.4	25.3	15.7	61.1	26.5	43.4
240 -- 360	77.8	13.6	55.2	11.8	23.5	14.6	70.9	30.2	42.5
360 -- 480	68.8	12.0	52.8	11.3	21.2	13.2	76.7	30.9	40.2
480 -- 600	55.6	9.7	47.5	10.1	17.9	11.1	85.3	32.2	37.7
600 -- 720	43.6	7.6	38.1	8.1	14.1	8.7	87.2	32.3	37.0
720 -- 840	37.8	6.6	32.5	6.9	11.8	7.3	85.9	31.2	36.3
840 -- 960	31.7	5.6	28.4	6.1	9.9	6.1	89.5	31.0	34.7
960 -- 1080	25.3	4.4	23.0	4.9	7.7	4.7	91.2	30.3	33.2
1080 -- 1200	21.0	3.7	19.3	4.1	6.3	3.9	92.2	30.1	32.7
Total	**571.7**	**100.0**	**468.8**	**100.0**	**161.2**	**100.0**			
Percent	**682.2**	**83.8**	**644.8**	**72.7**	**180.4**	**89.4**			

2.5 Model-validation results

The results of the validation test are shown in Figure S10. The model containing all variables showed the greatest similarity between the observed and simulated scenarios.
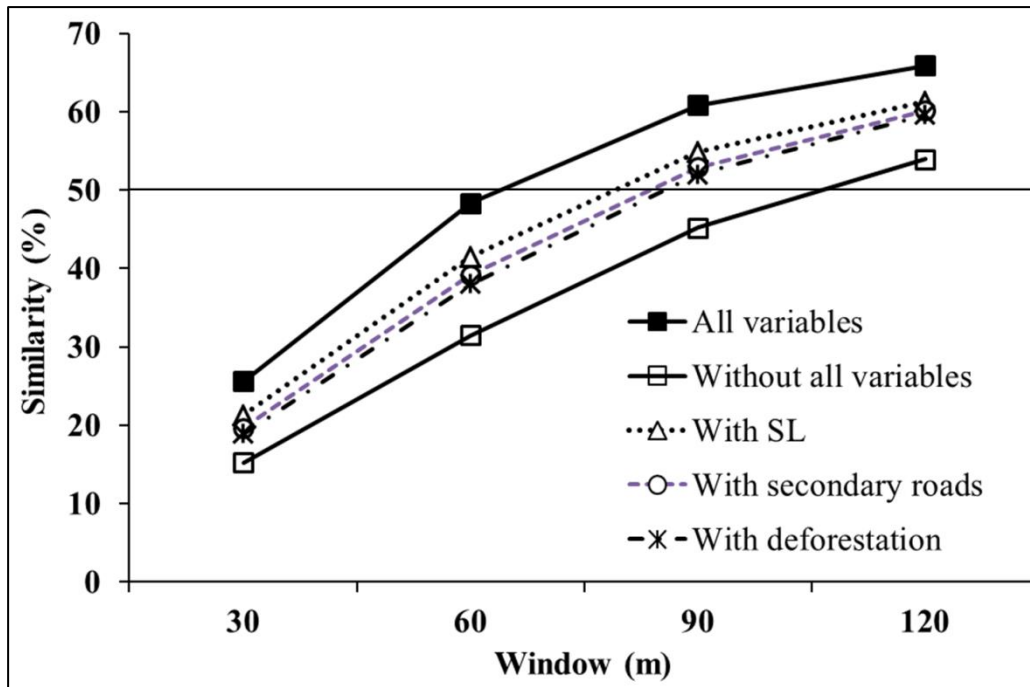
Figure S10. Similarity test between the modeled maps and the fire map for 2016.

2.6 Forest vulnerability to fire

The assessment of the vulnerability maps showed that the SL influenced the spread of fire in the study area during the 2015/2016 El Niño event. The exposure of forest areas to fires increased by 366.2% in the most-vulnerable range, which ranged from 79.11 to 99.99% (0.7911 to 0.9999 probability), with the presence of SL areas in the model compared to the absence of SL in the model (Table S16; Figures S11 and S12).

Table S16. Classes of vulnerability of the forest to forest fires.

| Range	Whole area regardless of impacts		Without SL		Without secondary roads		Without deforestation	
	Area (km²)	%	Area (km²)	%	Area (km²)	%	Area (km²)	%
0.0004 - 0.1488	2,550.4	47.1	1,750.1	32.3	2,467.7	45.6	2,478.5	45.8
0.1489 - 0.3955	421.4	7.8	822.4	15.2	511.3	9.4	501.1	9.3
0.3956 - 0.6109	407.5	7.5	938.9	17.3	500.3	9.2	478.1	8.8
0.6110 - 0.7910	547.7	10.1	1,315.5	24.3	588.7	10.9	609.0	11.2
0.7911 - 0.9999	1,487.9	27.5	587.9	10.9	1,346.7	24.9	1,348.1	24.9
Total	**5,414.8**	**100.0**	**5,414.8**	**100.0**	**5,414.8**	**100.0**	**5,414.8**	100.0
Range	Without SL, roads or deforestation		With SL		With secondary roads		With deforestation	
	Area (km²)	%	Area (km²)	%	Area (km²)	%	Area (km²)	%
0.0004 - 0.1488	1,576.3	29.1	1,859.3	34.3	1,557.9	28.8	1,497.2	27.7
0.1488 - 0.3955	784.3	14.5	821.7	15.2	966.9	17.9	985.9	18.2
0.3956 - 0.6109	694.7	12.8	671.2	12.4	707.8	13.1	802.0	14.8
0.6110 - 0.7910	2,045.3	37.8	912.2	16.8	735.8	13.6	951.1	17.6
0.7911 - 0.9999	314.2	5.8	1,150.4	21.2	1,446.4	26.7	1,178.6	21.8
Total	**5,414.8**	**100.0**	**5,414.8**	**100.0**	**5,414.8**	**99.9**	**5,414.8**	100.0
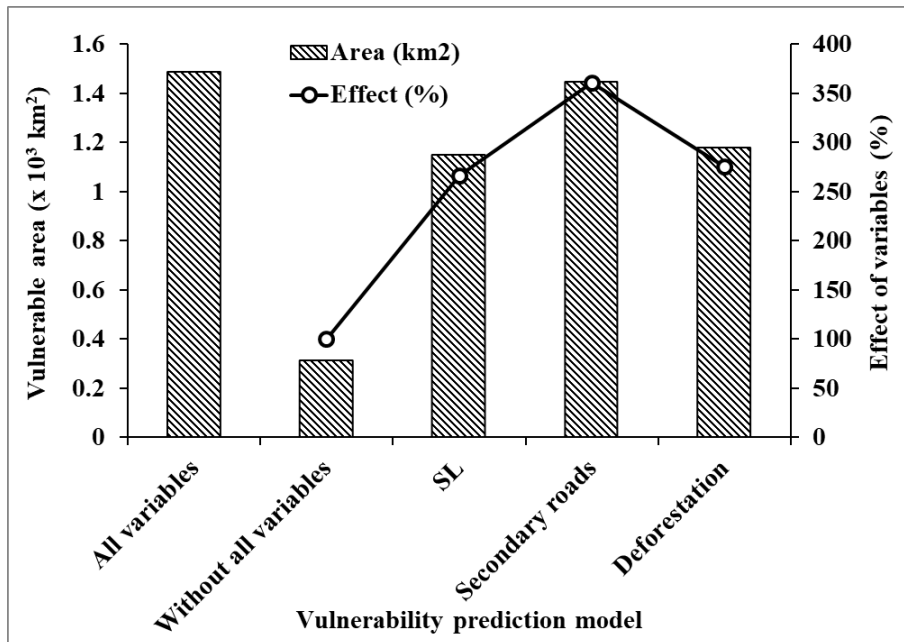
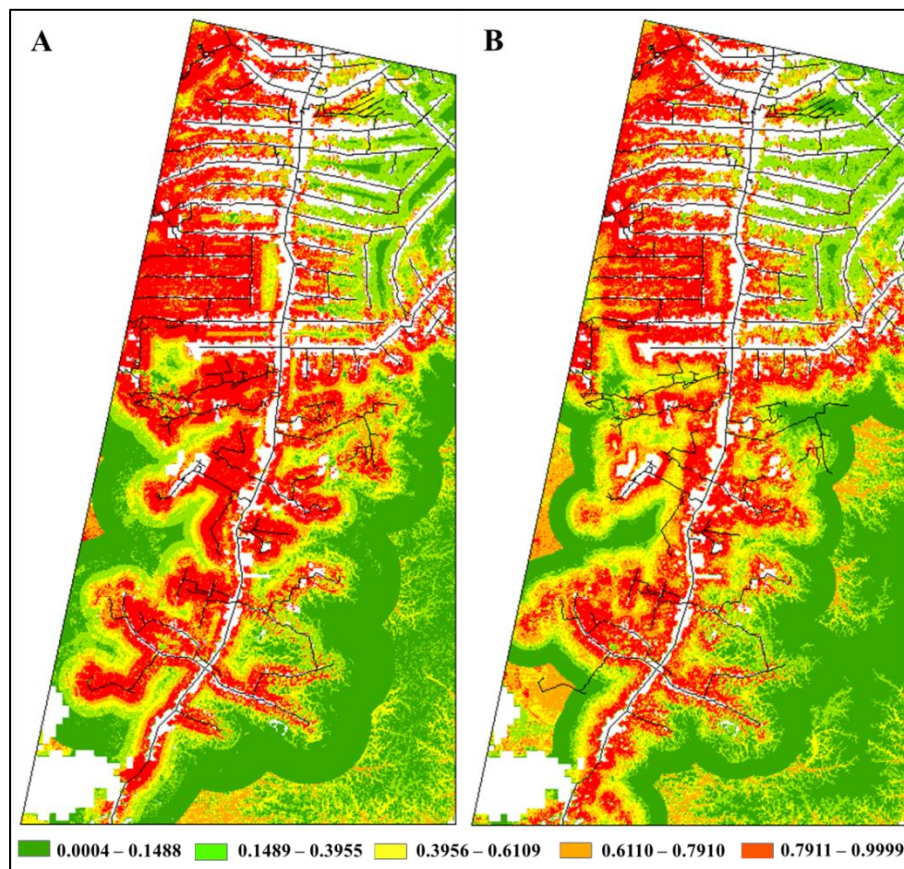**Figure S11.** Area vulnerable to understory forest fires in the study area.

Figure S12. Maps of the vulnerability of the forest to understory fires. (A) forest-vulnerability map calculated from variables not correlated with "secondary roads," plus the "secondary roads" variable and (B) forest-vulnerability map calculated from variables not correlated with "deforestation," plus the "deforestation" variable. The legend below the figure shows the ranges of probability ([0.1]) of the forest being affected by fire.
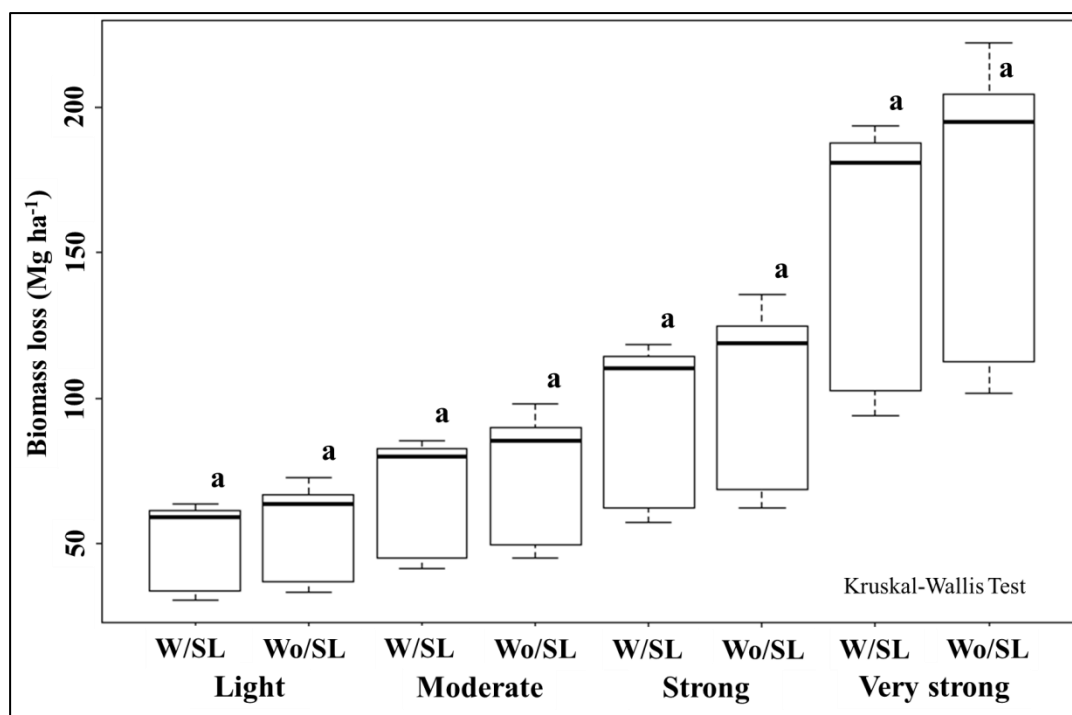
Figure S-13. Biomass loss (Mg ha^{-1}) by fire-severity class in areas with SL (W/SL) and areas without SL (Wo/SL) considering all forest types in the study area. The lower-case letters above the boxes indicate that there was no significant difference ($p < 0.05$) between the loss of biomass by fire in previously logged areas and unlogged areas within each severity class.

References

Barni, P.E., Fearnside, P.M., Graça, P.M.L.A., 2015. Simulating deforestation and carbon loss in Amazonia: impacts in Brazil's Roraima state from reconstructing Highway BR-319 (Manaus-Porto Velho). Environmental Management, 55, 124–1138. http://rd.springer.com/article/10.1007%2Fs00267-015-0447-7

Barni, P.E., Silva, E.B.R., Silva, F.C.F., 2017. Incêndios florestais de sub-bosque na zona de florestas úmidas do sul de Roraima: Área atingida e biomassa morta. In: Anais do Simpósio Brasileiro de Sensoriamento Remoto 2017. Campinas, SP, Brazil: Galoá, pp. 6280-6287. Available at: https://bityl.co/5JeV. Accessed on: 21 November 2020.

Bonham-Carter, G., 1994. Geographic Information Systems for Geoscientists: Modeling with GIS. Pergamon, New York, USA. 398 pp.

Brazil, IBGE (Instituto Brasileiro de Geografia e Estatística), 2021. Produção da Extração Vegetal e da Silvicultura: Tabela289. Available at: https://sidra.ibge.gov.br/Tabela/289. Accessed on: 19 March 2021.

Brazil, INPE (Instituto Nacional de Pesquisas Espaciais), 2020. Projeto PRODES – Monitoramento da Floresta Amazônica por Satélite. São José dos Campos, SP, Brazil: INPE. Available at: https://bityl.co/5JeS. Accessed on: 21November 2020.

da Silva, R.P., 2007. Alometria, Estoque e Dinâmica da Biomassa de Florestas Primárias e Secundárias na Região de Manaus (AM). Ph.D. Thesis in tropical forest science, Instituto Nacional de Pesquisas da Amazônia (INPA), Manaus, Amazonas, Brazil. https://repositorio.inpa.gov.br/bitstream/1/4966/1/Roseana_Silva.pdf

Fearnside, P.M., 1995. Global warming response options in Brazil's forest sector: Comparison of project-level costs and benefits. Biomass and Bioenergy, 8(5), 309-322. https://doi.org/10.1016/0961-9534(95)00024-0

Fearnside, P.M., 1997. Wood density for estimating forest biomass in Brazilian Amazonia. Forest Ecology and Management, 90(1), 59-89. https://doi.org/10.1016/S0378-1127(96)03840-6

Figueiredo Filho, D.B., Silva Junior, J.A., 2009. Desvendando os mistérios do coeficiente de correlação de Pearson (r). Política Hoje, 18(1), 115-146. https://periodicos.ufpe.br/revistas/politicahoje/article/view/3852/3156

Higuchi, N., Santos, J., Ribeiro, R.J., Minette L., Biot, Y., 1998. Biomassa da parte aérea da vegetação da floresta tropical úmida de terra-firme da Amazônia brasileira. Acta Amazonica, 28(2), 153-166. https://doi.org/10.1590/1809-43921998282166

Nogueira, E.M., Nelson, B.W., Fearnside, P.M., 2005. Wood density in dense forest in central Amazonia, Brazil. Forest Ecology and Management, 208(1-3), 261-286. https://doi.org/10.1016/j.foreco.2004.12.007

Nogueira, E.M., Fearnside, P.M., Nelson, B.W., Barbosa, R.I., Keizer, E.W.H., 2008. Estimates of forest biomass in the Brazilian Amazon: New allometric equations and adjustments to biomass from wood-volume inventories. Forest Ecology and Management, 256(11), 1853-1857. https://doi.org/10.1016/j.foreco.2008.07.022

Saldarriaga, J.G., West, D.C., Tharp, M., Uhl, C., 1988. Long-term chronosequence of forest succession in the upper Rio Negro of Colombia and Venezuela. Journal of Ecology,76, 938–958. https://doi.org/10.2307/2260625

Silveira, L.H.C., Rezende, A.V., Vale, A.T., 2013. Teor de umidade e densidade básica da madeira de nove espécies comerciais amazônicas. Acta Amazonica, 43(2), 179–184. https://doi.org/10.1590/S0044-59672013000200007

Soares-Filho, B.S., Ferreira, B.M., Filgueira, D.S., Rodrigues, H.O., Hissa, L.B.V., Lima, L.S., Machado, R.F., Costa, W.L.S., 2014. Dinamica project. Remote Sensing Center. Federal University of Minas Gerais (UFMG), Belo Horizonte, Minas Gerais, Brazil. Available at: http://www.csr.ufmg.br/dinamica/. Last access: 12 June 2020.